Excitation and emission enhancement of single molecule fluorescence through multiple surface-plasmon resonances on metal trimer nanoantennas

V. Giannini and J. A. Sánchez-Gil*

Instituto de Estructura de la Materia, Consejo Superior de Investigaciones Científicas, Serrano 121, 28006 Madrid, Spain

**Corresponding author: j.sanchez@iem.cfmac.csic.es*

Received December 14, 2007; revised February 19, 2008; accepted February 24, 2008; posted March 21, 2008 (Doc. ID 90901); published April 21, 2008

We study theoretically the light scattering from trimers of metal nanowires, with emphasis on the occurrence of multiple surface-plasmon resonances, showing that such resonances can be exploited to achieve twofold-enhanced fluorescence from a single molecule placed in the nanotrimer gaps, even if excitation and emission frequencies are separated. Pump enhancement stems from the local field enhancement coinciding with one of the resonances, whereas a strong enhancement of the radiative decay rate (and quantum yield) is revealed at a different resonance, leading to a large overall signal emission. © 2008 Optical Society of America

OCIS codes: 260.2510, 240.6680, 290.5850, 160.4236.

Metal nanoparticles exhibit a rich optical phenomenology owing to the excitation of surface-plasmon resonances (SPRs). These resonances stem from the oscillations of free electrons, inducing a dipole with a resonance frequency typically in the visible [1]. Besides larger scattering and absorption cross sections, such SPRs lead to high local field enhancements in a near-field region around the particle. In recent years, advances in nanofabrication techniques have made feasible a great variety of nanoparticle configurations, which have in turn fueled interest in surface-plasmon localization in metal nanostructures [2].

In this regard, if the nanoparticles present complex shapes and/or form (optically coupled) dimers, SPRs may become stronger; remarkably, extremely large near-field enhancements arise at resonance [3–15]. The concept of optical nanoantennas has been indeed coined to stress the ability of nanoparticles to convert visible light into localized electromagnetic energy and vice versa [8–10,16–18]. Furthermore, it has been experimentally shown that spontaneous emission is substantially enhanced at resonance when the emitters are located in the antenna gap, as a result of a remarkable increase in the electromagnetic local density of states [18,19].

It should be mentioned, however, that in all these works a single SPR is excited either at the pump frequency or at the emission frequency, so that the resulting SPR-mediated enhancement occurs only at one of the involved frequencies [except of course in the case of surface-enhanced Raman scattering (SERS), for which the corresponding Raman shift is typically so small that both frequencies may lie within a single SPR]. In this work we propose to use metal nanotrimers, based on dimer nanoantennas with another nanoparticle of different shape orientation in between, to exploit the resulting SPRs to enhance single-molecule fluorescence. To that end, calculations of the scattering cross section of nanotrimers have been carried out that illustrate the occurrence of strong SPRs at different frequencies. Near-field maps at resonant frequencies are shown, so that local enhancement factors can be given. Assuming that a fluorescent molecule is located nearby, the enhancement of the corresponding decay rates are investigated, along with the total enhancement of the resulting signal.

The physical system we consider is the following [see inset in Fig. 1(a)]. It consists of three Au nanowires (two-dimensional particles, i.e., particles having a translational symmetry along one direction), placed close to each other. The nanotrimer is illuminated in the plane of the figure with a p-polarized, monochromatic plane electromagnetic wave of frequency ω at an angle θ_0 with respect to the perpendicular to the trimer axis. The polarization is defined as shown; the magnetic field for p polarization (TM) is parallel to the nanowire invariant direction. Light-scattering calculations are based on the Green's theorem surface integral equation formulation, modified to deal with surface profiles in parametric form [20]. The dielectric constant of Au is obtained from [21].

In particular, we study the light scattering from a nanotrimer consisting of a 20 nm diameter cylinder located between two symmetrically placed triangular nanowires; each triangular cross section has a 20 nm base and 20 nm height, oriented so that the triangle base is perpendicular to the trimer axis, with the tip pointing toward the circle. The distance between the triangle tips and the cylinder is 5 nm. The electromagnetic field impinges perpendicular to the trimer axis; the corresponding scattering cross section (SCS) is shown in Fig. 1(a), along with the SCSs of the isolated triangle and the cylinder. It is seen that the resonance of each isolated nanowire is present also in the trimer SCS, but the coupling induces both a large redshift of the triangle main resonance and a slight blueshift of the cylinder main resonance. The former

0146-9592/08/090899-3/$15.00

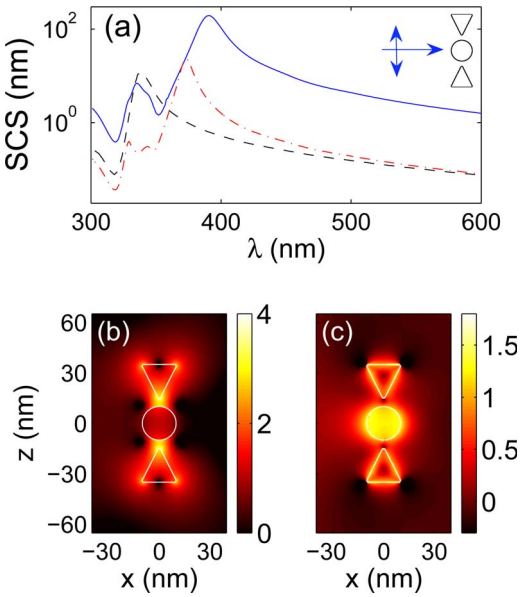

Fig. 1. (Color online) (a) Scattering cross section for a Ag trimer (solid curve) consisting of a cylinder with 20 nm of diameter between two triangles; each triangle has 20 nm of base and 20 nm of height. The distance between each triangle and the cylinder is 5 nm, the electromagnetic field impinging from the left (see inset), p polarization. SCS of a Ag triangular particle (dashed-dotted curve) and of a cylinder (dashed curve). (b), (c) Near electric field intensity in a $\log_{10}$ scale (p polarization) at the plasmonic resonances, normalized to that of the incident field. (b) $\lambda=390$ nm, (c) $\lambda=334$ nm.

redshift can be understood in terms of the hybridization [22], or the strong coupling [6], of bonding parallel modes; the latter blueshift is very small and indeed more difficult to interpret, since the corresponding cylinder main resonance is very weakly coupled to the adjacent triangles, as revealed below by the near-field maps. Note that all three nanowires have the same geometric cross section length (20 nm), but the SCS at the main resonance of the trimer is larger than that of the triangle main resonance multiplied by three.

In Figs. 1(b) and 1(c) we show the electric near-field intensity maps at the two trimer resonances. For the stronger resonance at $\lambda_2 \approx 390$ nm in Fig. 1(b), large electric field intensities appear at all triangle corners, but the bigger enhancement is observed in the two gaps between the triangle corners and the cylinder ($\sim 10^4$ times the incident field). This SPR is similar to that for bow-tie antennas [9,18], slightly shifted owing to the presence of the cylindrical inclusion. At $\lambda_1 \approx 334$ nm [see Fig. 1(c)], on the other hand, we can see that the electric field intensity is larger inside the cylinder, indeed quite similar to the pattern associated to the isolated cylinder resonance [12,20]. Actually, the presence of the two triangles barely alters this SPR, probably owing to the weak overlap between the near field with the triangular tips. Incidentally, higher-order multipolar resonances can be excited for single nanowires, as with the quadrupole mode of the single triangle [5] observed in Fig. 1(a) at ~ 330 nm, which could also be exploited for local field enhancement, albeit constrained by its strength, spectral range, and weak overlap with other dipolar resonances.

The strong bow-tie-like SPR can be used to enhance inelastic optical processes with negligible frequency shift, such as SERS (or even fluorescence in some cases), both at the excitation and emission frequency. However, in the case of frequency shifts larger than the SPR half-width, or even nonlinear processes, the interplay of at least two SPRs can be exploited. In addition, the local areas where the near-field intensity is enhanced at the two SPR frequencies should overlap. To illustrate this, let us assume that a fluorescent molecule is placed in the gap between the triangles and the cylinder, with an absorption peak at λ_1 and an emission band centered around λ_2. If the molecule–nanotrimer system is illuminated at λ_1, a pump enhancement proportional to the local field intensity $|\mathbf{E}(\lambda_1)|^2$ is triggered. The spontaneous emission at λ_2 is in turn driven by the bow-tie-like SPR. We calculate the modification of the decay rate in Fig. 2 on the basis of the classical dipole model [23–25]

$$\frac{\gamma}{\gamma_0} = 1 + \frac{3\eta_0 c^3}{2p_0^2\omega^3}\Im[\mathbf{p}_0^* \cdot \mathbf{E}(\mathbf{r}_0,\lambda_2)], \qquad (1)$$

where $\gamma_0 = \gamma_{r,0} + \gamma_{nr,0}$ is the intrinsic molecular decay rate, with radiative and nonradiative components, and $\eta_0 = \gamma_{r,0}/\gamma_0$ is the intrinsic quantum yield. In Eq. (1), the local field scattered by the presence of the nanotrimer at the position of the dipole, $E(\mathbf{r}_0,\lambda_2)$, is numerically calculated by means of the Green's theorem surface integral equations as in [19]; radiative and nonradiative contributions are obtained.

The resulting decay rates are shown in Fig. 2 for two dipole orientations and varying positions along

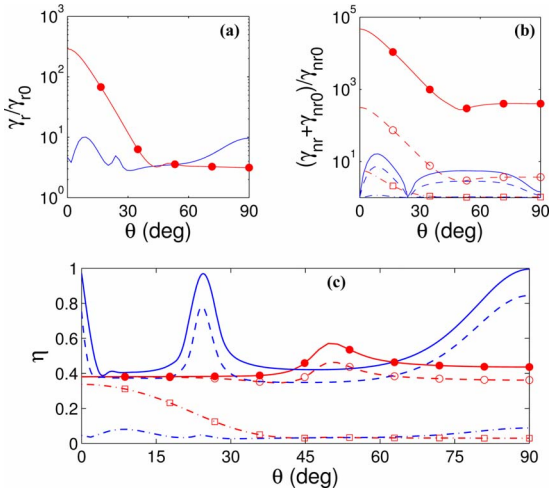

Fig. 2. (Color online) Normalized (a) radiative and (b) nonradiative decay rates and (c) quantum yield of an emitter placed at a constant distance of 2.5 nm from the cylinder of the nanotrimer shown in Fig. 1, at $\lambda=390$ nm (main SPR), for varying angles from $\theta=0°$ (center of one the trimer gaps) to 90°: dipoles oriented along either parallel (with symbols) or perpendicular (without symbols) to the dimer axis with intrinsic quantum yields of $\eta_0=99\%$ (solid curves), $\eta_0=40\%$ (dashed curves), and $\eta_0=1\%$ (dashed-dotted curves).

an arc of 90° separated 2.5 nm from the cylinder surface ($\theta=0°$ corresponds to the trimer axis). The radiative decay rate is strongly enhanced ($\gamma_r/\gamma_{r,0}\gtrsim 300$) when the dipole is located in the gap between the triangles and the cylinder and is oriented along the dimer axis; in contrast, the perpendicular dipole is only (weakly) enhanced at $\theta=90°$. Note that the enhancement is independent of the intrinsic quantum yield. The nonradiative decay rate is also enhanced, with enhancement factors strongly dependent on the intrinsic quantum yield. For the parallel dipole, the qualitative behavior of $1+\gamma_{nr}/\gamma_{nr,0}$ is similar to that of $\gamma_r/\gamma_{r,0}$, with maximum enhancement at $\theta=0°$ (in between the nanoparticles); nonetheless, the enhancement factors are larger the larger is η_0, reaching nearly 5 orders of magnitude for $\eta_0=99\%$. For the perpendicular dipole, the nonradiative decay rates are weakly enhanced overall and exhibit minima both at $\theta=0°$ and $\theta\sim 24°$, similar to the radiative decay rate and stemming from the particular near-field pattern associated with the strong SPR.

The corresponding apparent quantum yields $\eta \equiv \gamma_r/(\gamma_r+\gamma_{nr}+\gamma_{nr,0})$ are plotted in Fig. 2(c). For the molecules with large intrinsic quantum yields ($\eta_0=99\%$), the apparent quantum yield is typically lower than η_0 owing to the increase of the nonradiative decay rate, with maxima associated basically with minima of $\gamma_{nr}/\gamma_{nr,0}$. A similar qualitative behavior is observed, as expected, for molecules with relative large intrinsic quantum yield $\eta_0=40\%$. However, in the case of low $\eta_0=1\%$, the nanotrimer can indeed lead to a substantial increase of the apparent quantum yield, driven by the strong enhancement of the radiative decay rate. Actually, the total fluorescence enhancement can be determined below saturation through the expression [25]

$$\frac{I}{I_0}=\frac{\eta(\lambda_2)}{\eta_0}|\mathbf{E}(\lambda_1)|^2, \tag{2}$$

which combines the excitation enhancement through the near-field intensity at λ_1, and the emission enhancement η/η_0 at λ_2. [It should be born in mind that, for the latter expression to be applicable, the dipole position and orientation must be taken into account upon calculating $\eta(\lambda_2)$ and $|\mathbf{E}(\lambda_1)|^2$.] The two SPRs associated with the nanotrimer give rise to enhancements both at the excitation wavelength [see Fig. 1(c)], with nearly 1 order of magnitude enhancement, and at the emission wavelength [see Fig. 2(c) for $\eta_0=1\%$, with $\eta/\eta_0\sim 30$], thus leading to single-molecule fluorescence enhancements of 2–3 orders of magnitude. This might be especially relevant for low-efficiency molecules [26].

In conclusion, metallic nanowire trimers have been investigated, exploring the rich phenomenology associated with multiple plasmon resonances. The enhanced local electromagnetic field associated with such SPRs can be exploited to doubly enhanced inelastic and/or nonlinear optical processes. As a proof of principle, we have shown that strong single-molecule fluorescence enhancements can be achieved with a trimer consisting of a bow-tie nanoantenna modified with a cylindrical nanoparticle in between, with straightforward implications for low efficiency emitters as in, e.g., (bio)molecular sensing or optoelectronic devices. A proper design of the nanotrimer can be exhaustively explored to maximize the twofold enhancement for the particular inelastic–nonlinear optical process of interest.

We acknowledge J. Gómez Rivas and O. Muskens for stimulating discussions. This work was supported in part by the Spanish DGI-MEC (grant FIS2006-07894) and the Comunidad de Madrid (grant S-0505/TIC-0191 and V. Giannini's Ph.D. scholarship).

References

1. U. Kreibig and M. Vollmer, *Optical Properties of Metal Clusters* (Springer, 1995).
2. W. L. Barnes, A. Dereux, and T. W. Ebbesen, Nature **424**, 824 (2003).
3. H. Xu, J. Aizpurua, M. Käll, and P. Apell, Phys. Rev. E **62**, 4318 (2000).
4. J. P. Kottmann, O. J. F. Martin, D. R. Smith, and S. Schultz, Phys. Rev. B **64**, 235402 (2001).
5. K. L. Kelly, E. Coronado, L. L. Zhao, and G. C. Schatz, J. Phys. Chem. B **107**, 668 (2003).
6. J. Aizpurua, G. W. Bryant, L. J. Richter, F. J. García de Abajo, B. K. Kelley, and T. Mallouk, Phys. Rev. B **71**, 235420 (2005).
7. P. Nordlander, C. Oubre, E. Prodan, K. Li, and M. I. Stockman, Nano Lett. **4**, 899 (2004).
8. D. P. Fromm, A. Sundaramurthy, P. J. Schuck, G. Kino, and W. E. Moerner, Nano Lett. **4**, 957 (2004).
9. P. J. Schuck, D. P. Fromm, A. Sundaramurthy, G. S. Kino, and W. E. Moerner, Phys. Rev. Lett. **94**, 017402 (2005).
10. P. Mühlschlegel, H. J. Eisler, O. J. F. Martin, B. Hecht, and D. W. Pohl, Science **308**, 1607 (2005).
11. K. L. Shuford, M. A. Ratner, and G. C. Schatz, J. Chem. Phys. **123**, 114713 (2005).
12. I. Romero, J. Aizpurua, G. W. Bryant, and F. J. García de Abajo, Opt. Express **14**, 9988 (2006).
13. S. E. Sburlan, L. A. Blanco, and M. Nieto-Vesperinas, Phys. Rev. B **73**, 035403 (2006).
14. T. Søndergaard and S. I. Bozhevolnyi, Opt. Express **15**, 4198 (2007).
15. V. Giannini, J. A. Sánchez-Gil, J. V. García-Ramos, and E. R. Méndez, Phys. Rev. B **75**, 235447 (2007).
16. J. J. Greffet, Science **308**, 1561 (2005).
17. L. Novotny, Phys. Rev. Lett. **98**, 266802 (2007).
18. L. Rogobete, F. Kaminski, M. Agio, and V. Sandoghdar, Opt. Lett. **32**, 1623 (2007).
19. O. Muskens, V. Giannini, J. A. Sánchez-Gil, and J. Gómez Rivas, Nano Lett. **7**, 2871 (2007).
20. V. Giannini and J. A. Sánchez-Gil, J. Opt. Soc. Am. A **24**, 2822 (2007).
21. P. B. Johnson and R. W. Christy, Phys. Rev. B **6**, 4370 (1972).
22. H. Wang, D. W. Brandl, P. Nordlander, and N. J. Halas, Acc. Chem. Res. **40**, 53 (2007).
23. R. R. Chance, A. Prock, and R. Silbey, Adv. Chem. Phys. **37**, 1 (1978).
24. R. Carminati, J.-J. Greffet, C. Henkel, and J. M. Vigoureux, Opt. Commun. **261**, 368 (2006).
25. P. Bharadwaj and L. Novotny, Opt. Express **15**, 14266 (2007).
26. J. R. Lakowicz, Anal. Biochem. **337**, 171 (2005).